Cell-type, Dose, and Mutation-type Specificity Dictate Mutant p53 Functions In Vivo

Ming Kei Lee,[1] Wei Wei Teoh,[1] Beng Hooi Phang,[1] Wei Min Tong,[2] Zhao Qi Wang,[3,4] and Kanaga Sabapathy[1,5,6,*]

[1]Division of Cellular and Molecular Research, Humphrey Oei Institute of Cancer Research, National Cancer Centre, 11, Hospital Drive, Singapore 169610, Singapore
[2]Institute of Basic Medical Sciences School of Basic Medicine, Chinese Academy of Medical Sciences, Peking Union Medical College 5, Dong Dan San Tiao, 100005, Beijing, China
[3]Leibniz Institute for Age Research, Fritz Lipmann Institute e.V., Beutenbergstrasse 11, 07745 Jena, Germany
[4]Biology and Pharmacy Faculty, Friedrich-Schiller-University, 07745 Jena, Germany
[5]Cancer and Stem Cell Biology Program, Duke-NUS Graduate Medical School, 8, College Road, Singapore 169857, Singapore
[6]Department of Biochemistry, National University of Singapore, 8, Medical Drive, Singapore 117597, Singapore
*Correspondence: cmrksb@nccs.com.sg
http://dx.doi.org/10.1016/j.ccr.2012.10.022

SUMMARY

The specific roles of mutant p53's dominant-negative (DN) or gain-of-function (GOF) properties in regulating acute response and long-term tumorigenesis is unclear. Using "knockin" mouse strains expressing varying R246S mutant levels, we show that the DN effect on transactivation is universally observed after acute p53 activation, whereas the effect on cellular outcome is cell-type specific. Reducing mutant p53 levels abrogated the DN effect. Mutant p53's DN effect protected against radiation-induced death but did not accentuate tumorigenesis. Furthermore, the R246S mutant did not promote tumorigenesis compared to $p53^{-/-}$ mice in various models, even when MDM2 is absent, unlike the R172H mutant. Together, these data demonstrate that mutant p53's DN property only affects acute responses, whereas GOF is not universal, being mutation-type specific.

INTRODUCTION

Mutations in *p53* occur in over 50% of all human cancers, and in the other cases, alterations in the p53 pathway have been observed, indicating that the functional inactivation of the p53 pathway is a critical step in tumor formation (Robles and Harris, 2010; Zilfou and Lowe, 2009). Most of the mutations are missense mutations—often in the DNA-binding domain—and therefore lead to loss of target gene transactivation (Olivier et al., 2010). Mutations in *p53* often occur during the course of tumorigenesis, and hence, the mutant allele coexists with the wild-type allele in the cell for a time period until the latter is lost because of loss-of-heterozygozity (LOH), leaving behind the mutant allele in some cancers (Levine et al., 1991; Robles and Harris, 2010). Mutant *p53* is also found in the germline in the case of Li-Fraumeni syndrome (LFS) patients, resulting in higher

rate of tumorigenesis. Interestingly, LOH is not observed in all LFS patients, suggesting that mutant p53 may exhibit dominant-negative (DN) activities or reduced p53 activity per se may be sufficient to drive carcinogenesis (haploid insufficiency) (Palmero et al., 2010; Varley et al., 1997). Regardless of the sporadic or familial nature of cancers, the observation of LOH of the wild-type allele in some cancers indicates that complete loss of wild-type p53 further promotes turmorigenesis, and cells expressing only mutant p53 may have additional advantages through acquired gain-of-functions (GOF) (Brosh and Rotter, 2009; Oren and Rotter, 2010).

A large body of in vitro work using overexpressed mutant p53 has demonstrated mutant p53's ability to bind and inhibit wild-type p53 activity when both coexist, in a phenomenon termed as the DN effect (Kern et al., 1992; Milner and Medcalf, 1991; Petitjean et al., 2007). However, the relevance of DN

Significance

Mutant p53 has been shown to exhibit dominant-negative (DN) effects and gain-of-function (GOF) properties in vitro, though the in vivo relevance is relatively unclear. Using knockin mouse strains expressing varying levels of the R246S mutant, we show that the DN effect is exhibited in vivo in a cell-type-specific and dose-dependent manner, being observed only after acute p53 activation and preventing radiosensitivity but not contributing to long-term tumorigenesis. GOF, however, was not observed in various cancer/cellular models, even when MDM2 is absent. These data therefore signify the need for the evaluation of p53 status during cancer therapy, which often activates p53 acutely, leading possibly to DN effects. Moreover, the GOF property appears not to be a universal phenomenon of p53 mutants.

activity in vivo in the context of tumor formation has been questionable. The initial generation of knockin mice and cells expressing mutant p53 has indicated that DN activity is displayed in some tissues, such as embryonic stem cells, breast and lung epithelium, but not in others, such as the skin epithelium, unless UV irradiated, indicating a contextual setting in which such activity can be manifested (Jackson et al., 2005; Lee and Sabapathy, 2008; Wijnhoven et al., 2005, 2007). However, detailed characterization of mutant p53's DN activity in multiple tissues after p53 activation and in the context of concomitant tumorigeneis has not been performed, and its significance is not well understood. Given that tumors would generally retain the wild-type allele in mutant p53 expressing cells in the early phases—during which chemo- and radiotherapies may be administered—the impact of mutant p53's DN effect can be expected to be a crucial factor in determining successful therapeutic and hence survival outcome. Studies on human follicular lymphoma have shown that heterozygote status with the presence of one mutant *p53* allele leads to poor overall survival and shortened time of disease progression (O'Shea et al., 2008), supporting this hypothesis.

Similarly, a substantial amount of evidence exists for the oncogenic GOF of mutant p53, which has been shown to be capable of transactivating novel noncanonical target genes that confer additional growth advantage, migratory potential, and drug resistance (Muller et al., 2009; Weisz et al., 2007, Yeudall et al., 2012). We and others have also demonstrated that cancer cells become addicted to mutant p53 expression, abrogation of which leads to cell death and reduced tumor formation in scid mice (Bossi et al., 2006; Vikhanskaya et al., 2007). Moreover, mutant p53 interacts with a variety of cellular proteins, such as p63, p73, and NF-Y, thereby altering the activities of these proteins to prevent proliferation or interfere with apoptosis (Oren and Rotter, 2010). Consistently, analysis of two strains of knockin mice expressing hot spot mutants R172H and R270H revealed that these mutants were capable of inhibiting p63/73 function, supporting the case for GOF (Lang et al., 2004; Olive et al., 2004). Subsequent experiments with other cancer models using these knockin mice confirmed this phenomenon (Jackson et al., 2005; Morton et al., 2010), elevating enthusiasm that all p53 mutants may generally exhibit GOF that could be amenable to therapeutic targeting. However, it remains unclear whether GOF is a universal property of all hot spot p53 mutants. Furthermore, the manifestation of GOF has been correlated to conditions in which mutant p53 is "hyperstable," such as in the "cancer-cell context" or in the absence of Mdm2, where basal mutant p53 levels are elevated, leading to enhanced spontaneous tumor formation (Terzian et al., 2008), suggesting a requirement for increased stability for phenotypic manifestation of GOF. However, current data are not conclusive enough to confirm the universality of this requirement.

Hence, we have embarked on addressing the role of DN and GOF in detail, through the use of knockin mice strains expressing different levels of the R246S mutant, equivalent of the hot spot human R249S mutant, to understand the effect of its presence in various tissues upon pathological and nonpathological p53 activating conditions, some of which lead to tumorigenesis over time.

RESULTS

Mutant p53 Exhibits Dominant Negative Effect on Cellular Viability in a Cell-type-Dependent Manner

To determine the effects of mutant p53 over its wild-type counterpart in an endogenous setting in various tissues, we generated a knockin mouse strain that carries the *R246S* mutation (human *R249S* equivalent) through germline targeting (Figure S1A available online) and analyzed a variety of cell types after exposure to γ-irradiation (IR) or treatment with the p53-activating agent nutlin (Vassilev et al., 2004). Whole-body irradiation showed that thymocytes were expectedly highly sensitive to IR in vivo and die in a p53-dependent manner, as $p53^{-/-}$ thymocytes were almost completely resistant to cell death (Figure 1A; Figure S1B). $p53^{+/-}$ thymocytes were also very sensitive, though less than $p53^{+/+}$ cells. By contrast, $p53^{+/R246S}$ thymocytes were significantly more resistant to death than $p53^{+/-}$ cells, being almost similar to $p53^{-/-}$ cells, indicating DN activity of the mutant protein over the wild-type protein (percentage of cell viability- $p53^{+/R246S}$ versus $p53^{+/-}$: 90.17 ± 4.22 versus 62.47 ± 1.76; p < 0.001) (Figure 1A). To confirm the cell-autonomous nature of this effect, we isolated thymocytes from various genotypes of mice and irradiated or treated them with nutlin ex vivo. Irradiation with 5 Gy and analysis over time indicated that $p53^{+/R246S}$ thymocytes were indeed more resistant than $p53^{+/-}$ (percentage of cell viability at 15 hr- $p53^{+/R246S}$ versus $p53^{+/-}$: 66.37 ± 3.11 versus 36.84 ± 1.45; p < 0.001) (Figure 1B). Similar results were obtained with various doses of irradiation (percentage of cell viability at 5 Gy- $p53^{+/R246S}$ versus $p53^{+/-}$: 62.70 ± 2.24 versus 33.86 ± 1.33; p < 0.001) (Figure 1C). Moreover, treatment with nutlin also led to the exhibition of DN effect of the mutant p53, as thymocytes from $p53^{+/R246S}$ mice were more resistant than $p53^{+/-}$ cells (percentage of cell viability at 15 hr- $p53^{+/R246S}$ versus $p53^{+/-}$: 45.52 ± 3.77 versus 19.50 ± 1.63; p < 0.001) (Figure 1D).

Detailed analysis of several lymphoid organs revealed that cell death was less pronounced in thymus, spleen, and lymph nodes of $p53^{+/R246S}$ mice compared to $p53^{+/-}$ mice after whole-body irradiation (Figure 1E). However, cell death was similar in bone marrow (BM) cells from these two genotypes. To confirm that DN effect is lacking in BM cells, we purified and used Lin^{-ve} progenitor cells from BM, which confirmed the lack of DN effect in this cell type (percentage of cell viability- $p53^{+/R246S}$ versus $p53^{+/-}$: 31.65 ± 3.34 versus 22.40 ± 2.40; p > 0.05) (Figure 1F). Thus, to determine if the DN effect seen in the other organs is attributable to specialized cell types, we analyzed T and B cells from lymph nodes and spleen after staining with anti-CD3 and anti-B220 antibodies, respectively. Ex vivo irradiation led to a significant DN effect in $p53^{+/R246S}$ CD3^{+ve} cells from both spleen and lymph nodes (p < 0.05) (Figure 1G). Similarly, nutlin treatment also led to DN effect in $p53^{+/R246S}$ CD3^{+ve} cells, in which cell death was less compared to their $p53^{+/-}$ counterparts (percentage of cell viability- $p53^{+/R246S}$ versus $p53^{+/-}$: 61.45 ± 3.38 versus 42.69 ± 2.46 for 10 μM nutlin; p < 0.001 and 53.73 ± 1.63 versus 33.69 ± 0.77 at 5 Gy, p < 0.001) (Figures 1H, S1C, and S1D). B220^{+ve} cells from $p53^{+/R246S}$ mice were also significantly more resistant to cell death than $p53^{+/-}$ cells upon nutlin treatment and irradiation, though the difference was less pronounced at a higher dose of irradiation (percentage of cell
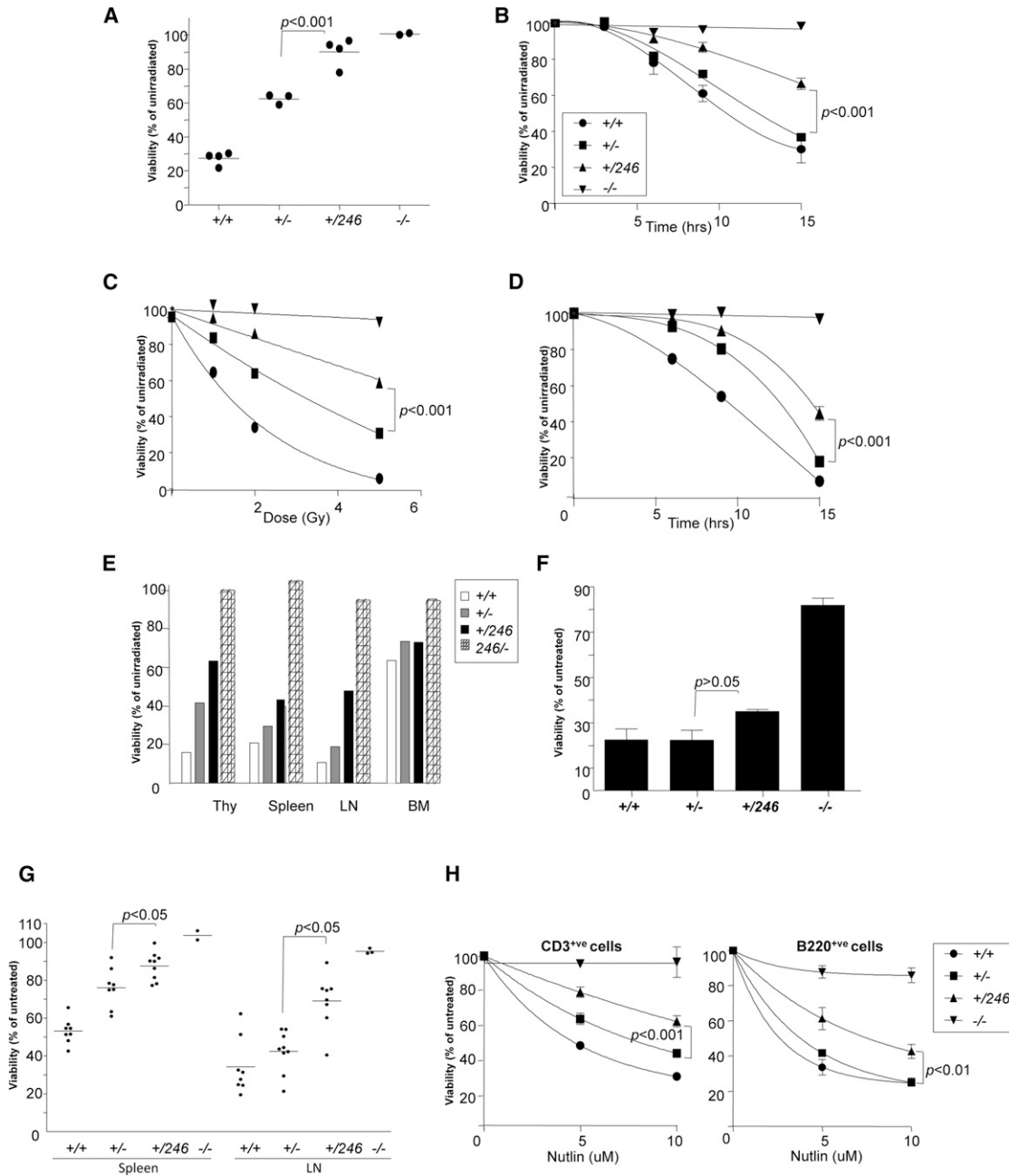
Figure 1. DN Effect of Mutant p53 on Cell Death Is Cell-type Specific

(A) Thymocytes of whole-body irradiated (5 Gy) 5-week-old mice were harvested 12 hr later for flow cytometric determination of viability after annexin-V/propidium iodide (PI) staining. Mean viability for each genotype (–) and thymocyte viability of each individual mouse (●) are shown.

(B–D) Thymocytes were irradiated ex vivo (5 Gy or otherwise indicated) (B and C) or treated with 10 μM nutlin (D) for 15 hr (or otherwise indicated), and cellular viability was determined by normalizing against unirradiated samples for each time point. Data represents mean ± SEM with 2–8 mice/genotype.

(E–H) Thymocytes, splenocytes, lymph node (LN), and bone marrow (BM) cells were irradiated (5 Gy) ex vivo (E–G) or treated with nutlin (H), and viability was determined 12–15 hr later. Lineage negative (Lin⁻ᵛᵉ) cells were purified from BM and assayed similarly (F). Viability of CD3⁺ᵛᵉ and B220⁺ᵛᵉ cells were determined by staining with FITC-annexin-V and PE-conjugated CD3 or B220 antibody double staining, respectively, followed by flow cytometric analysis (G, CD3⁺ cells only) and (H, CD3⁺ or B220⁺ cells). Mean viability (–) for each genotype and the viability of cells from each individual mouse (●) are represented by dots (G). Data represents mean ± SEM with three mice/genotype.

See also Figure S1.

viability- *p53*⁺/R246S versus *p53*⁺/⁻: for nutlin, 61.24 ± 6.33 versus 41.73 ± 2.00 at 5 μM, p < 0.001; and 42.52 ± 4.01 versus 25.06 ± 2.37 at 10 μM, p < 0.01 and 47.54 ± 0.89 versus 29.53 ± 1.61 at

2 Gy, p < 0.01; and 17.84 ± 0.21 versus 10.61 ± 0.17 at 5 Gy) (Figures 1H and S1C). Collectively, these results demonstrate the cell-type-specific exhibition of DN effect of mutant p53.
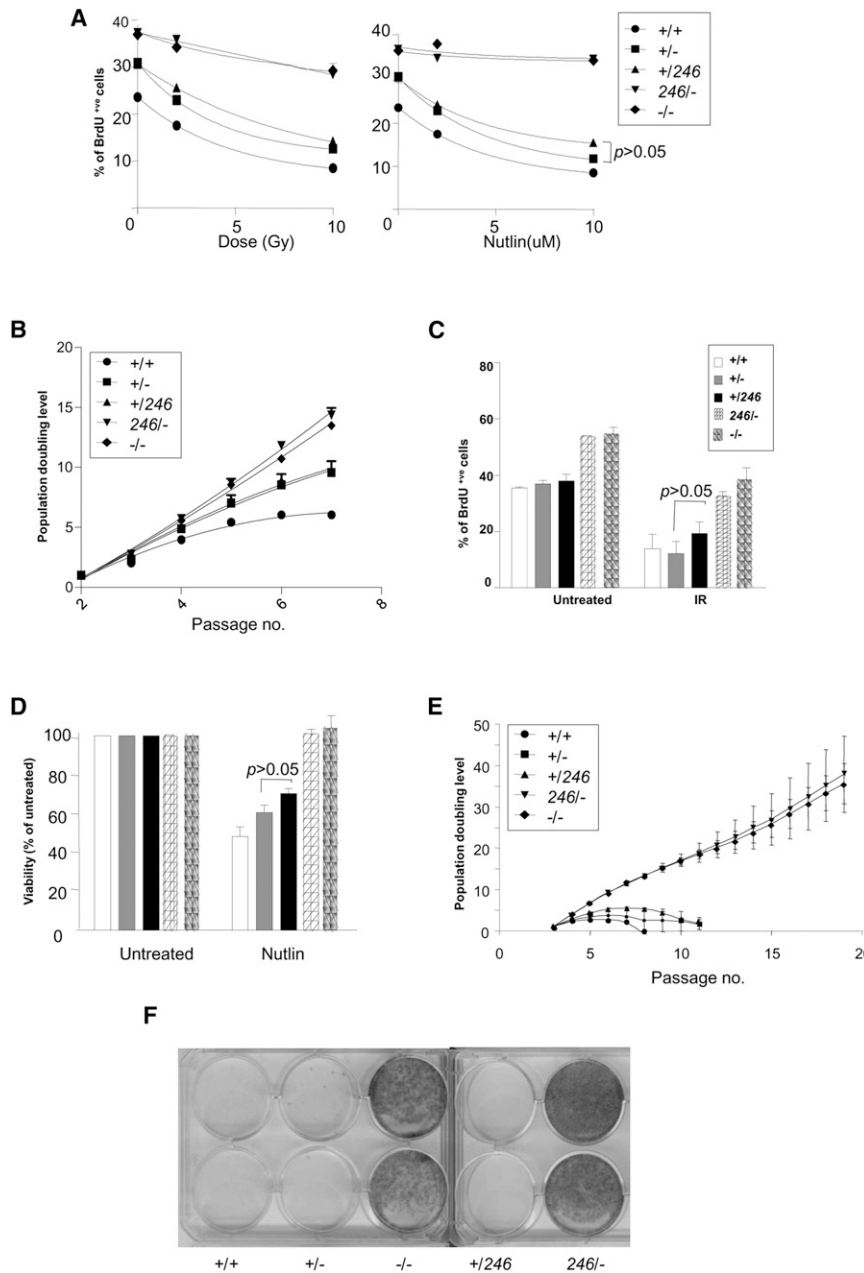
Figure 2. Cellular Predisposition to Cell Death or Cell-Cycle Arrest Does Not Dictate Mutant p53's DN Effect

(A) Primary MEFs (same passage) of different *p53* genotypes were γ-irradiated or nutlin treated and pulsed with 10 μM BrdU 24 hr after treatment for 1 hr. BrdU^{+} cells were detected by flow cytometric analysis.

(B) Growth potential of primary MEFs was determined by population doubling in culture over seven passages. Data represents mean ± SEM with 3–4 clones of MEFs/genotype.

(C and D) Early passage E1A/Ras-transformed MEFs were γ-irradiated (5 Gy) or nutlin treated (10 mM), and the proportion of BrdU^{+} cells was determined (C). Cell death of E1A/Ras-transformed MEFs was determined by annexin-V/PI staining (D). Data represents mean ± SEM with 3–4 mice/genotype.

(E) Spontaneous transformation/replicative senescence of primary MEFs was determined by growing cells in accordance with the 3T3 protocol. Data represents mean ± SEM with two clones of MEFs/genotype.

(F) Primary MEFs were transduced with oncogenic mutant Ras-V12-expressing retrovirus and selected for 2 weeks with puromycin. Viable cell colonies were stained with crystal violet, and representative data of three independent replicates are shown.
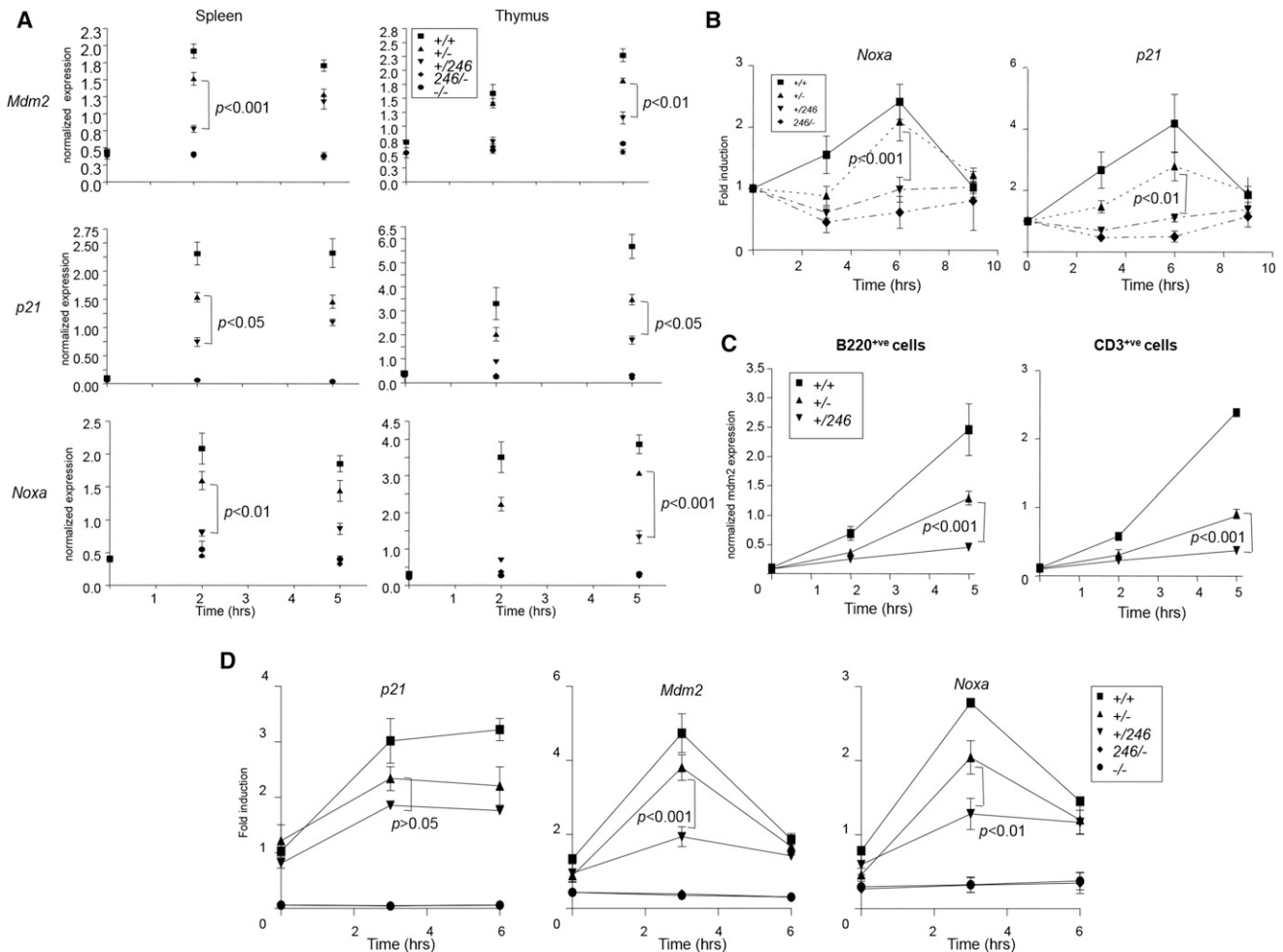
Moreover, growth rates were similar between *p53[+/R246S]* fibroblasts and *p53^{+/−}* cells and lower than the *p53^{−/−}* cells (Figure 2B). As primary fibroblasts generally undergo cell-cycle arrest upon irradiation, we utilized MEFs that have been transformed by the expression of E1A+Ras oncogenes, which have been shown to sensitize MEFs to cell death (Lowe et al., 1993). E1A/Ras-transformed *p53[+/R246S]* fibroblasts did not also exhibit any significant DN effects upon irradiation on cellular proliferation (percentage of BrdU incorporation-*p53[+/R246S]* versus *p53^{+/−}*: 19.40 ± 4.00 versus 12.24 ± 4.36; p > 0.05) (Figure 2C) or cell death (percentage of cell viability- *p53[+/R246S]* versus *p53^{+/−}*: 70.38 ± 2.59 versus 60.52 ± 3.86; p > 0.05) (Figure 2D). Basal BrdU incorporation for primary and E1A/Ras-transformed MEFs were also not significantly different (*p53[+/R246S]* versus *p53^{+/−}*: primary - 30.70 ± 1.21 versus 30.93 ± 0.43; p > 0.05 and E1A/Ras - 38.00 ± 2.43 versus 36.95 ± 1.25; p > 0.05) (Figures 2A and 2C). These data indicate that lack of DN effect in MEFs is regardless of their predisposition to cell-cycle arrest (primary MEFs) or death (transformed cells).

We next explored the DN potential during cellular senescence and transformation in MEFs. Primary MEFs were grown in the 3T3 protocol and development of spontaneous transformation was assayed. As shown in Figure 2E, *p53^{−/−}* and *p53[R246S/-]* cells

Lack of DN Effect Is Not due to Cellular Predisposition to Cell Death or Cellular Senescence

As the DN effect on cellular survival appears to be only seen in some cell types, we utilized primary mouse embryonic fibroblasts (MEFs) to determine DN effects on cellular proliferation and senescence. Treatment with nutlin or irradiation led to a reduction in BrdU incorporation in a p53-dependent manner (Figure 2A). However, *p53[+/R246S]* fibroblasts were as sensitive as the *p53^{+/+}* and *p53^{+/−}* cells, suggesting that the mutant p53 does not have a negative effect of the remaining wild-type protein (percentage of Brdu incorporation- *p53[+/R246S]* versus *p53^{+/−}*: 14.33 ± 0.22 versus 12.63 ± 0.24; p > 0.05 at 10 Gy and 15.53 ± 0.56 versus 11.75 ± 0.09; p > 0.05 at 10 μM nutlin).

Figure 3. DN Effect of Mutant p53 on Transactivation of p53-Target Genes

(A) Various tissues from whole-body irradiated (10 Gy) mice were harvested at the times indicated for determination of p53 target gene expression by quantitative real-time RT-PCR (normalized against actin). Data represents mean ± s.e.m. with 4-8 mice/genotype, except where only 2 $p53^{-/-}$ mice were used.

(B) Thymocytes were irradiated (5Gy) ex vivo prior to analysis of p53 target genes. Fold induction was calculated based on unirradiated samples. Data represents mean ± s.e.m. with 4-8 mice/genotype, except where only 2 $p53^{246/-}$ mice were used.

(C) CD3$^+$ and B220$^+$ cells from spleens of 6-8 week old mice were purified and irradiated (5Gy) prior to determination of expression of p53 target genes. Data represents mean ± SEM with 2–3 mice/genotype.

(D) Early passage (<passage 4) MEFs of different $p53$ genotypes were irradiated (10 Gy), and p53 target gene expression was determined. Data represents mean ± SEM with 3–4 mice/genotype.

readily transformed spontaneously in culture without undergoing replicative senescence, whereas $p53^{+/+}$, $p53^{+/-}$, and $p53^{+/R246S}$ MEFs did not, suggesting that the R246S mutant is incapable of exhibiting DN effects to overcome barriers of transformation. In addition, we utilized oncogenic Ras to induce oncogene-induced senescence, which again revealed the lack of DN effect, as only $p53^{-/-}$ and $p53^{R246S/-}$ cells were transformed, unlike the others (Figure 2F), demonstrating the absence of a DN effect during both spontaneous and Ras-induced senescence/transformation of MEFs in culture.

These data together demonstrate that the coexistence of endogenous mutant p53 and wild-type p53 leads to a DN effect on p53-mediated cell survival only in some cell types upon p53 activation.

Mutant p53 Exhibits DN Effect on p53-Mediated Transactivation in Both Sensitive and Insensitive Cell Types

We next examined if p53-mediated target gene transactivation is sensitive to DN effects of mutant p53 in various cell types by performing quantitative real-time PCR analysis. Whole-body irradiation led to maximal p53 target gene activation around 2 hr in spleen and 5 hr in thymus (Figure 3A). *Mdm2*, *p21*, and *Noxa* levels were highest at these time points, respectively, in the $p53^{+/+}$ case, whereas it was slightly reduced in $p53^{+/-}$ cells. However, target gene activation was significantly reduced in tissues from the $p53^{+/R246S}$ mice, almost similar to the $p53^{-/-}$ case (Figure 3A). It is noteworthy that the difference between $p53^{+/-}$ and $p53^{+/R246S}$ cases were maximal and significant at

the highest point of activation (normalized *Mdm2* expression - $p53^{+/-}$ versus $p53^{+/R246S}$: 1.512 ± 0.094 versus 0.776 ± 0.050 for spleen, p < 0.001 and 1.814 ± 0.041 versus 1.148 ± 0.108 for thymus, p < 0.01; *p21* expression - 1.534 ± 0.085 versus 0.741 ± 0.077 for spleen, p < 0.05 and 3.466 ± 0.219 versus 1.781 ± 0.166 for thymus, p < 0.05; *Noxa* expression - 1.590 ± 0.136 versus 0.799 ± 0.050 for spleen, p < 0.01 and 3.073 ± 0.027 versus 1.324 ± 0.178 for thymus, p < 0.001).

p53 target gene activation in thymocytes and purified T and B cells from spleen after irradiation ex vivo was also examined. Similar to the in vivo case, p53-dependent *p21* and *Noxa* activation was maximal around 6 hr after irradiation in thymocytes, at which point the difference between $p53^{+/-}$ and $p53^{+/R246S}$ was most obvious and significant (normalized *Noxa* expression - $p53^{+/-}$ versus $p53^{+/R246S}$: 2.088 ± 0.313 versus 0.982 ± 0.205, p < 0.001; *p21* expression - 2.787 ± 0.468 versus 1.110 ± 0.135, p < 0.01) (Figure 3B). Importantly, these targets were minimally activated in $p53^{+/R246S}$ cells. Purified T and B cells also showed a similar trend, where the *Mdm2* activation was markedly reduced in $p53^{+/R246S}$ cells compared to $p53^{+/-}$ cells (normalized *Mdm2* expression - $p53^{+/-}$ versus $p53^{+/R246S}$: 1.288 ± 0.116 versus 0.450 ± 0.053, p < 0.001 for B220$^+$ cells; 0.739 ± 0.068 versus 0.369 ± 0.032, p < 0.001 for CD3$^+$ cells at 5 hr) (Figure 3C), highlighting that the presence of mutant p53 was indeed affecting the wild-type p53-dependent target gene activation in sensitive cells.

Because we noted the absence of a DN effect on cell death and proliferation in MEFs, we evaluated if p53-dependent target gene activation is at all affected by the presence of mutant p53. Whereas *p21* activation was not compromised in $p53^{+/R246S}$ MEFs, indicating the lack of a DN effect, *Noxa* and *Mdm2* activation was significantly compromised (normalized *Mdm2* expression - $p53^{+/-}$ versus $p53^{+/R246S}$: 3.808 ± 0.344 versus 1.934 ± 0.267, p < 0.001; *Noxa* expression – 2.044 ± 0.224 versus 1.280 ± 0.210, p < 0.01; *p21* expression – 2.341 ± 0.215 versus 1.858 ± 0.009, p > 0.05 at 3 hr) (Figure 3D). *Mdm2* and *Noxa* activation in $p53^{+/R246S}$ MEFs was minimal and significantly lower than in $p53^{+/-}$ cells. These data indicate that the DN effect on transactivation can indeed be observed in MEFs on some target genes, despite the lack of effect on the biological outcome (Figure 2). Altogether, the data highlight that the DN effect of mutant p53 on wild-type p53-mediated transactivation is observed in both sensitive tissues, such as thymus and lymphoid cells, and selectively on some target genes in insensitive cells, like the MEFs.

Threshold Level of Mutant p53 Is Required for DN Effect In Vivo

Another knockin mouse strain that carries the same R246S mutation but which also retains the neomycin resistance cassette in intron 6 of the *p53* locus, therefore making it a potential hypomorphic allele ($p53^{+/R246SNeo}$) (Figure S2), was generated. Analyzing transcript levels revealed that the mutant *p53* levels were considerably lower in $p53^{+/R246SNeo}$ thymocytes compared to $p53^{+/R246S}$ thymocytes (Figure 4A). Irradiation of thymocytes and splenocytes led to an increase in total p53 levels in cells from all *p53* genotypes but was maximal in the $p53^{+/R246S}$ case (Figure 4B). By contrast, p53 levels were lower in $p53^{+/R246SNeo}$ cells, confirming that the mutant p53 is indeed expressed at

a higher steady-state level and that the presence of the neomycin cassette leads to a hypomorphic state, resulting in reduced expression (Figure 4B).

Irradiation of thymocytes revealed that the cells from $p53^{+/R246SNeo}$ mice were as sensitive as the $p53^{+/-}$ cells and not as resistant as the $p53^{+/R246S}$ cells, suggesting a lack of the DN effect in the $p53^{+/R246SNeo}$ case (percentage of cell viability at 5 Gy- $p53^{+/R246S}$ versus $p53^{+/R246Sneo}$: 62.50 ± 3.03 versus 45.71 ± 1.75, p < 0.001) (Figure 4C). To confirm if this loss of the DN effect on cell viability is also observed on p53-target gene transactivation, *p21* and *Noxa* induction was analyzed. As shown in Figure 4D, both the target genes were induced to a greater extent in the $p53^{+/R246SNeo}$ cells, compared to the $p53^{+/R246S}$ cells that showed minimal activation. Importantly, the level of induction was comparable between $p53^{+/R246SNeo}$ cells and $p53^{+/-}$ cells, thereby confirming the lack of a DN effect in the former cells (normalized *p21* expression - $p53^{+/-}$ versus $p53^{+/R246SNeo}$ versus $p53^{+/R246S}$ 3.042 ± 0.188 versus 3.168 ± 0.114 versus 1.666 ± 0.124, p > 0.05 for $p53^{+/-}$ versus $p53^{+/R246Neo}$ and p < 0.001 for $p53^{+/-}$ versus $p53^{+/R246S}$; *Noxa* expression – 4.757 ± 0.35 versus 4.203 ± 0.465 versus 0.712 ± 0.21, p > 0.05 for $p53^{+/-}$ versus $p53^{+/R246SNeo}$ and p < 0.001 for $p53^{+/-}$ versus $p53^{+/R246S}$, at 5 hr). Similar results were obtained using splenocytes on cellular viability (percentage of cell viability at 5 Gy- $p53^{+/R246S}$ versus $p53^{+/R246SNeo}$: 71.439 ± 4.104 versus 43.591 ± 1.545, p < 0.001) (Figure 4E) and target gene activation (normalized *Mdm2* expression - $p53^{+/-}$ versus $p53^{+/R246SNeo}$ versus $p53^{+/R246S}$ 1.608 ± 0.307 versus 1.618 ± 0.329 versus 0.891 ± 0.074, p > 0.05 for $p53^{+/-}$ versus $p53^{+/R246SNeo}$ and p < 0.01 for $p53^{+/-}$ versus $p53^{+/R246S}$; *p21* expression – 1.883 ± 0.244 versus 1.832 ± 0.237 versus 0.790 ± 0.082, p > 0.05 for $p53^{+/-}$ versus $p53^{+/R246SNeo}$ and p < 0.001 for $p53^{+/-}$ versus $p53^{+/R246S}$, at 5 hr) (Figure 4F). These data together demonstrate that a threshold level of mutant p53 expression is required for the manifestation of DN effects, below which the effect is abrogated.

Mutant p53's DN Effect Affects Acute Response but Does Not Accentuate Tumor Formation

Low-dose (≤5 Gy) whole-body irradiation sensitizes p53 heterozygous mice to tumor formation (lymphomas and thymomas) (Kemp et al., 1994). Hence, we investigated if the DN effect on cellular survival seen in thymocytes and lymphocytes can lead to accentuation of tumor formation after low-dose whole-body irradiation. Analysis of CD3^{+ve} cell count from peripheral blood a day after irradiation showed a reduction in mice of all *p53* genotypes, although the decrease appeared to be less pronounced in $p53^{+/R246S}$ mice and almost negligible in p53$^{-/-}$ mice (Figure 5A). To analyze this effect in detail, we performed a time-course analysis of CD3^{+ve} cell numbers, which showed a dramatic decrease in cell numbers following the first day after irradiation, but which recovered starting from about day 4 onward (Figure 5A). The decrease was most significant in $p53^{+/+}$ mice, followed by the $p53^{+/-}$ mice. However, the decrease was less pronounced in $p53^{+/R246S}$ and $p53^{-/-}$ mice, indicative of DN activity during the acute response phase of radiosensitivity (for 24 hr after whole-body irradiation, absolute count of CD3$^+$ cells/μl of peripheral blood - $p53^{+/R246S}$ versus $p53^{+/-}$: 2,190.42 ± 60.10 versus 1,065.67 ± 164.00, p < 0.05). It is noteworthy that the
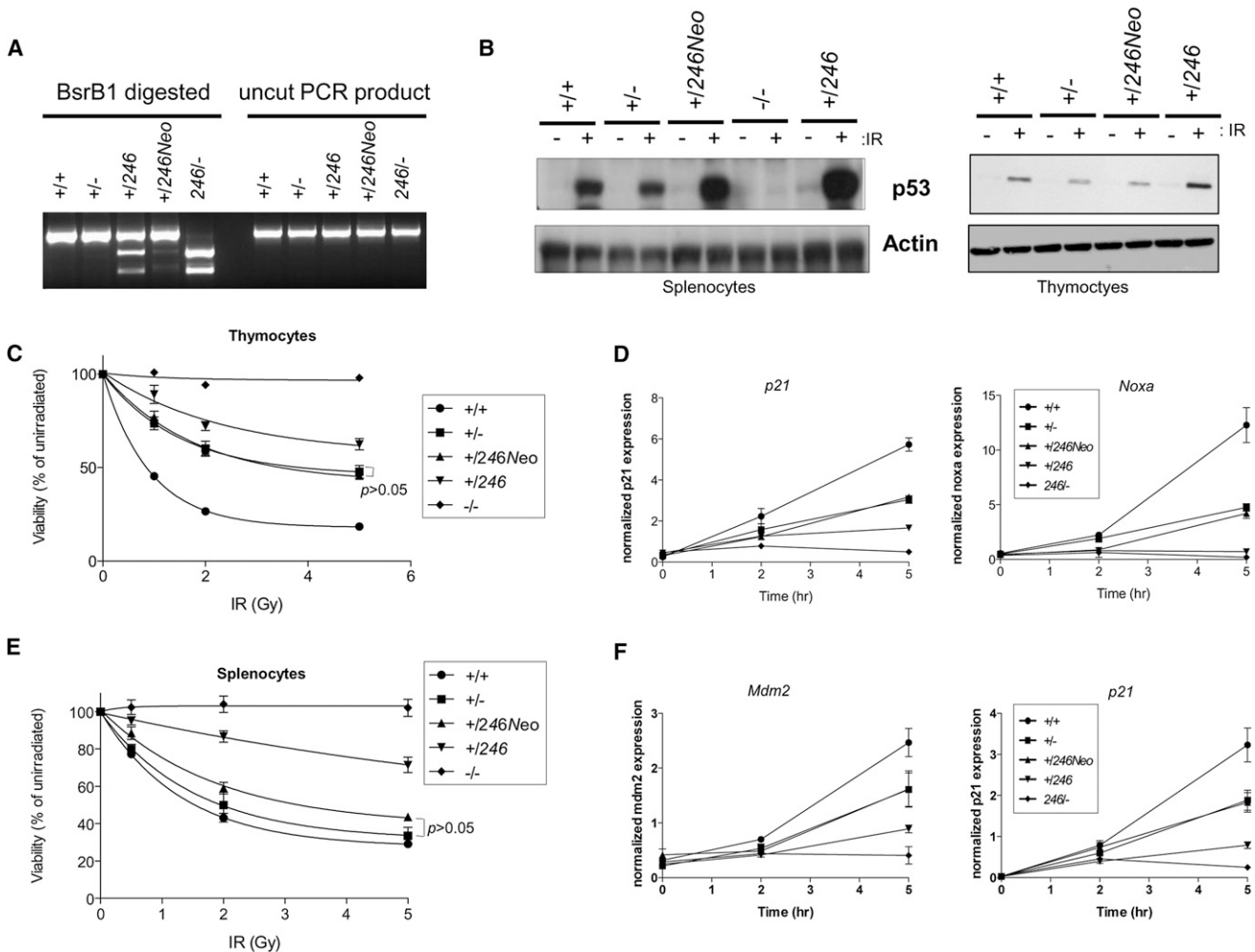
Figure 4. DN Effects Are Abrogated in Hypomorphic Mutant p53-Expressing p53$^{+/R246SNeo}$ Mice

(A) Expression of different *p53* alleles was determined by restriction fragment length polymorphism using thymocyte cDNA. *p53* transcript was amplified by RT-PCR, and 1 μg of purified RT-PCR product was digested with the *BsrB1* restriction enzyme—because of the generation of this site by the introduced R246S mutation—and analyzed by agarose gel electrophoresis. The relative intensity of the cleaved products indicates the expression levels of the knockin allele.

(B) Irradiated (5 Gy) splenocytes and thymocytes were harvested, and p53 protein levels were determined by immunoblotting. Representative blot of two independent experiments are shown.

(C–F) Viability of thymocytes (C) and splenocytes (E) was determined after irradiation. Expression of p53 target genes after irradiation (5 Gy) of thymocytes (D) and splenocytes (F) were determined. Data represents mean ± SEM with 3–4 (C and E) or 2–3 (D and F) mice/genotype, except for the *p53*$^{-/-}$ case in which one mouse was used for thymocytes. p values are shown for differences between the *p53*$^{+/246Neo}$ and *p53*$^{+/-}$ genotypes.

See also Figure S2.

numbers returned to almost baseline levels about 2 weeks after irradiation and that there was no elevation beyond the baseline values in both in *p53*$^{+/R246S}$ and *p53*$^{-/-}$ mice (Figure 5A).

Long-term monitoring of these irradiated cohorts of mice expectedly led to thymoma/lymphoma/sarcoma formation in a p53-dependent manner (median tumor-free survival of *p53*$^{+/-}$ versus *p53*$^{-/-}$ mice is 33.43 weeks versus 16.65 weeks, p < 0.01) (Figure 5B). However, tumor formation rate was not accentuated in *p53*$^{+/R246S}$, which were almost identical to the *p53*$^{+/-}$ case (median tumor-free survival of *p53*$^{+/R246S}$ versus *p53*$^{+/-}$ mice is 35.43 weeks versus 33.43 weeks, p = 0.835), indicating that the initial DN effect on cell death after acute DNA damage did not have any impact on tumor formation rates. Analysis of

tumor spectrum revealed that majority of both *p53*$^{+/R246S}$ and *p53*$^{+/-}$ mice developed sarcomas primarily and lymphomas to a lesser extent (data not shown), confirming the lack of DN effect on carcinogenesis.

To further confirm that the mutant p53-mediated DN effect is indeed only observed at the initial acute phase but is not contributory to tumor formation, we utilized the Myc-induced B cell lymphoma model (*Eμ-Myc* transgenics) to follow the fate of B cells that develop lymphomas in a p53-dependent manner (Schmitt et al., 1999). First, we purified B cells from *Eμ-Myc* transgenic mice of the various *p53* genotypes at an early age, where LOH has not taken place (Figures S3A and S3B), to determine the effect of irradiation. The analysis revealed that the
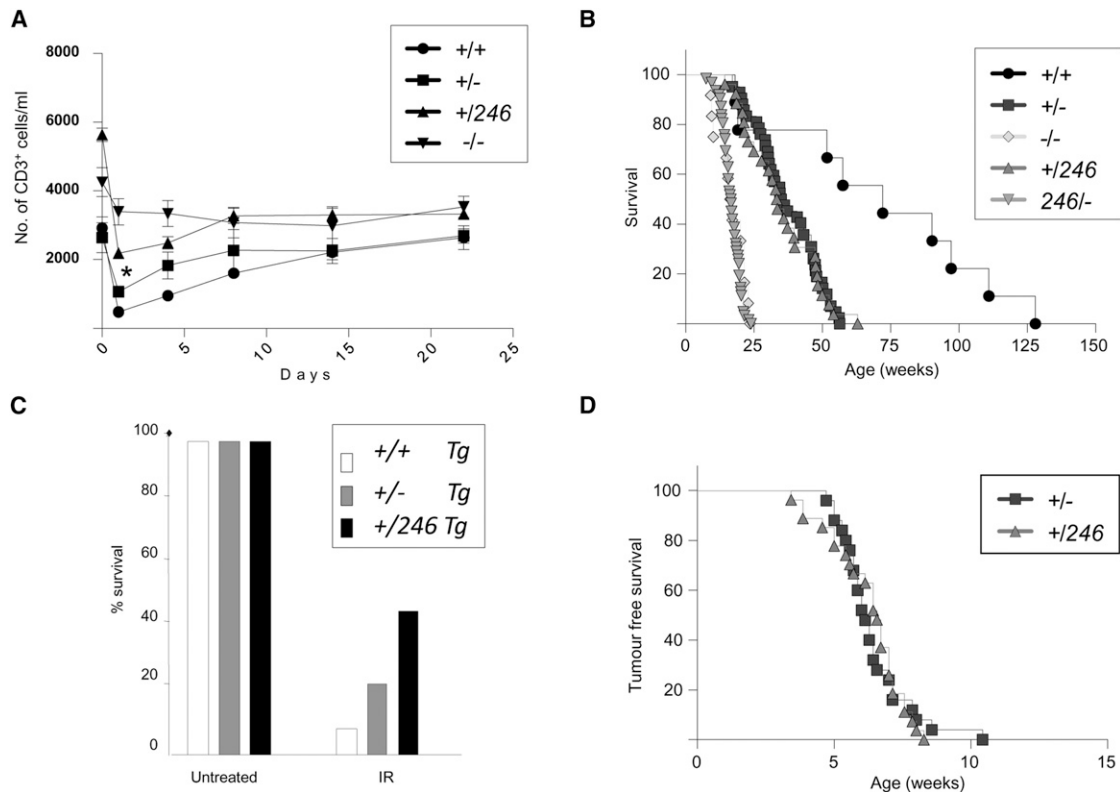
Figure 5. DN Effect Contributes to Acute p53-Mediated Response but Does Not Promote Tumorigenesis

(A) Absolute counts of peripheral CD3^{+} lymphocytes from 20 μl of blood collected from 8-week-old mice were determined before and up to 3 weeks after whole-body γ-irradiation (2.5 Gy). Data represents mean ± SEM with three mice/genotype. * represents $p < 0.05$ for differences between the $p53^{+/246}$ and $p53^{+/-}$ genotypes.

(B) Kaplan-Meier survival curves of γ-irradiated (single dose, at 5–8 weeks) mice are shown.

(C) B220^{+} cells were purified from splenocytes of 4 weeks old Eμ-Myc transgenic mice of various p53 genotypes and irradiated (5 Gy), prior to determination of cellular viability. Data represents the percent viability normalized against unirradiated control.

(D) Kaplan-Meier survival curves of Eμ-Myc transgenic mice of various p53 genotypes are shown.

See also Figure S3.

presence of the mutant protein led to resistance to cell death compared to the $p53^{+/-}$ cells (percentage of cell viability-$p53^{+/R246S}$ versus $p53^{+/-}$: 42.26 versus 20.29 with Myc) (Figure 5C), indicating the presence of DN activity on cellular survival upon acute p53 activation. Monitoring these mice over time indicated that both the $E\mu$-$Myc;p53^{+/R246S}$ mice and $E\mu$-$Myc;p53^{+/-}$ mice succumbed to tumor formation at the same rate, with the median tumor-free survival being 6.57 and 6.14 weeks, respectively (p = 0.973) (Figure 5D). These results suggest that the DN effect seen after acute p53 activation on cell death during the radiosensitive phase does not lead to enhanced tumorigenesis.

DN Effect Is neither Exhibited during Spontaneous Tumor Formation in the Absence of Stress Stimuli nor Evident during Embryonic Lethality Because of Mdm2 Absence

In order to further investigate if a DN effect is exhibited in the absence of exposure to acute stress signals, we first monitored a cohort of mice of various p53 genotypes for spontaneous tumor formation. Similar to the irradiated cohorts, the median survival of $p53^{+/-}$ and $p53^{+/R246S}$ mice was comparable,

indicating a lack of DN effects on overall tumorigenesis (median survival of $p53^{+/-}$ and $p53^{+/R246S}$ mice: 63.43 versus 59.86 weeks, p = 0.46) (Figure 6A; Table 1). Furthermore, there was no difference in the spectrum of tumors arising from mice of $p53^{+/-}$ and $p53^{+/R246S}$ genotypes (comparison of tumor spectrum by genotype, $p53^{+/-}$ versus $p53^{+/R246S}$ mice: 2 lymphoma and 19 sarcoma versus 8 lymphoma and 15 sarcoma, p = 0.0725 by Fisher's exact test) (Table 1). However, when we focused on the incidence of lymphoma alone, there is a slight but statistically significant decrease in the lymphoma incidence in $p53^{+/R246S}$ mice (lymphoma-bearing $p53^{+/R246S}$ versus $p53^{+/-}$ mice: 2/20 versus 8/19, p = 0.031 by Fisher's exact test) (Table 1). Nonetheless, there was no significant difference in survival between $p53^{+/-}$ and $p53^{+/R246S}$ mice in terms of spontaneous or IR-induced tumor formation, as well as in the $E\mu$-Myc lymphoma model (Figure 5; Table 1), suggesting that though the DN effect of mutant p53 may affect the type of cancers because of cell-type specificity, it does not affect overall tumor susceptibility. Supporting this idea, no significant difference was noted in the lymphoma incidence between the $p53^{+/R246S}$ versus $p53^{-/-}$ mice (lymphoma-bearing $p53^{+/R246S}$

versus $p53^{-/-}$ mice: 8/19 versus 29/42, p = 0.054, Fisher's exact test), although the rate of tumorigenesis was markedly different between the genotypes (Table 1), indicating that the mutant allele may have an effect on tissue specificity, though not having any DN effect on overall tumorigenesis.

Second, we investigated if embryonic lethality due to Mdm2 deficiency—that can be rescued by inactivation of p53 (Jones et al., 1995)—can be rescued by the DN effect of mutant p53. To that end, we intercrossed the $p53^{+/R246S};Mdm2^{+/-}$ double heterozygotes and found no viable $Mdm2^{-/-}$ mice with $p53^{+/+}$ or $p53^{+/R246S}$ genotypes, in contrast to $Mdm2^{-/-};$ $p53^{R246S/R246S}$ double homozygous mice, which were viable at birth (number of $Mdm2^{-/-};p53^{+/+}$, $Mdm2^{-/-};p53^{+/R246S}$, and $Mdm2^{-/-};p53^{R246S/R246S}$ mice found at the time of weaning: 0, 0, and 22, respectively) (Table 2). These results indicated that the R246S mutant is a completely nonfunctional mutant, reflecting the $p53^{-/-}$ case when homozygous but does not confer DN effects to rescue $Mdm2^{-/-}$ lethality.

These data therefore show that the DN effect of mutant p53 is only manifested during the acute p53 activation phase and does not contribute in any significant way to accelerate tumor formation in the three models studied here, as well as during embryogenesis.

Elevated Mutant p53 Expression in the Absence of Mdm2 or in Tumors Is Insufficient to Confer GOF Properties

We next explored if the R246S mutant possesses oncogenic GOF properties, by first analyzing the tumor formation rates in several models. As shown in Figure 5B and Figure 6A, the median survival of $p53^{-/-}$, $p53^{R246S/-}$, and $p53^{R246S/R246S}$ mice are comparable during both spontaneous and IR-induced cancer formation (spontaneous cancers - $p53^{-/-}$ versus $p53^{R246S/-}$ versus $p53^{R246S/R246S}$: 21.29 versus 20.86 versus 19.71 weeks, p = 0.375, for IR-induced cancer $p53^{-/-}$ versus $p53^{R246S/-}$: 16.64 versus 16.5 weeks, p = 0.23), suggesting that the R246S mutant may not possess GOF properties. Detailed analysis indicated that the $p53^{-/-}$, $p53^{R246S/-}$, and $p53^{R246S/R246S}$ mice developed mainly lymphomas and sarcomas with similar incidence, much more than the $p53^{+/R246S}$ and $p53^{+/-}$ mice, during both spontaneous and IR-induced cancer formation (proportion of $p53^{-/-}$ versus $p53^{R246S/R246S}$ mice developing spontaneous tumors that are lymphoma and sarcoma: 69% and 23.9% versus 78.3% and 21.7%, p = 0.3846 by Fisher's exact test) (Table 1 and data not shown). Unlike the case of other hot spot mutant p53 - R172H, metastasis was not observed in the tumor-bearing $p53^{R246S/-}$ and $p53^{R246S/R246S}$ mice (data not shown), further suggesting a lack of GOF properties of the R246S mutant.

Terzian and colleagues have suggested that the manifestation of the GOF of mutant p53 can be elevated by increasing the abundance of the mutant p53 protein, in the $Mdm2^{-/-}$ background (Terzian et al., 2008). To investigate this aspect, we first analyzed the status of mutant p53 in normal thymus and thymoma of $p53^{R246S/-}$ mice by immunoblotting, which indicated that the stabilization of the protein only in the tumorigenic state (Figure 6B), similar to the observation with other hot spot mutant p53 knockin mice (Lang et al., 2004; Olive et al., 2004). Immunohistochemical staining of tumors of $p53^{R246S/R246S}$ mice also confirmed the elevation of R246S mutant protein only in tumor

cells (Figures S4A–S4D), altogether implying that the abundance of R246S mutant in tumors alone is insufficient to confer GOF. Moreover, the stabilized mutant p53 was found to be S18 phosphorylated (Figure 6B), suggesting elevated basal DNA damage in tumors that may contribute to its increased abundance.

We thus evaluated if the R246S mutant p53 would be capable of exhibiting GOF properties in the $Mdm2^{-/-}$ background, by generating cohorts of $p53^{R246S/R246S}$ mice with different $Mdm2$ genotypes. As shown in Figure 6C, the median survival of $p53^{R246S/R246S}$ mice with different $Mdm2$ genotypes were similar (median survival of $p53^{R246S/R246S}$ mice with $Mdm2$ genotypes +/+ versus +/− versus −/−: 16 versus 17.5 versus 17.57 weeks, p = 0.577). Analysis of the tumor spectrum of these mice also revealed no significant differences among the various $Mdm2$ genotypes, suggesting that the R246S mutant does not possess oncogenic GOF properties (proportion of $Mdm2^{+/+}$ versus $Mdm2^{+/-}$ versus $Mdm2^{-/-}$ mice with $p53^{R246S/R246S}$ harboring lymphoma: 71.4% versus 54.2% versus 58.3% and sarcoma: 28.6% versus 37.5% versus 25%, p = 0.9039 by chi-square test) (Table S1A). Examination of mutant p53 expression in normal tissues (spleen and thymus) revealed that the level of R246S mutant protein was indeed elevated in the absence of Mdm2 (Figure 6D, left panel). Furthermore, the R246S mutant protein levels were much higher in tumors compared to normal tissues lacking Mdm2 (Figure 6D, right panel), implying that phosphorylation of mutant p53 in the tumor context may prevent its degradation. Immunohistochemical staining of tumors of $p53^{R246S/R246S}$; $Mdm2^{-/-}$ mice also confirmed the elevated levels of R246S mutant in tumors and in normal tissues (Figures S4E–S4H). These data therefore indicate that elevation of mutant p53 levels alone by Mdm2 absence or by the DNA damage context in tumors is insufficient to confer GOF properties to the R246S mutant.

GOF Is a Phenomenon Exhibited by the R172H Mutant but Not by the R246S Mutant

Although we did not observe any biological differences between $p53^{-/-}$ and $p53^{R246S/R246S}$ mice with and without Mdm2, one cannot exclude the possibility that there may be subtle differences that cannot be revealed by macroscopic analysis. Transcriptome profiling was thus performed using normal thymus from $p53^{-/-}$ and $p53^{R246S/R246S}$ mice with/without Mdm2. The principal component analysis (PCA) of normal thymi indicated the transcriptome profiles were nearly identical among different genotypes (data not shown). In order to detect differential gene expression based on different $p53$ genotypes, we performed ANOVA and compared the transcriptomes of $p53^{-/-}$ and $p53^{R246S/R246S}$ samples. As shown by the volcano plot in Figure S4I (left panel), most genes showed high p values and low fold changes, suggesting they are not significantly differentially expressed, indicating the lack of GOF in normal tissues. A similar trend was also noted in the absence of Mdm2, implying that Mdm2 loss per se does not confer GOF to the R246S mutant p53 (Figure S4I, right panel).

To determine if the "tumor context" is a prerequisite for the manifestation of GOF, we performed additional microarray analyses using B cells (primary or $E\mu$-myc-induced lymphoma) and MEFs (E1A/Ras transformed). For B lymphoma analysis, only cells that have lost the wild-type allele were used so that the
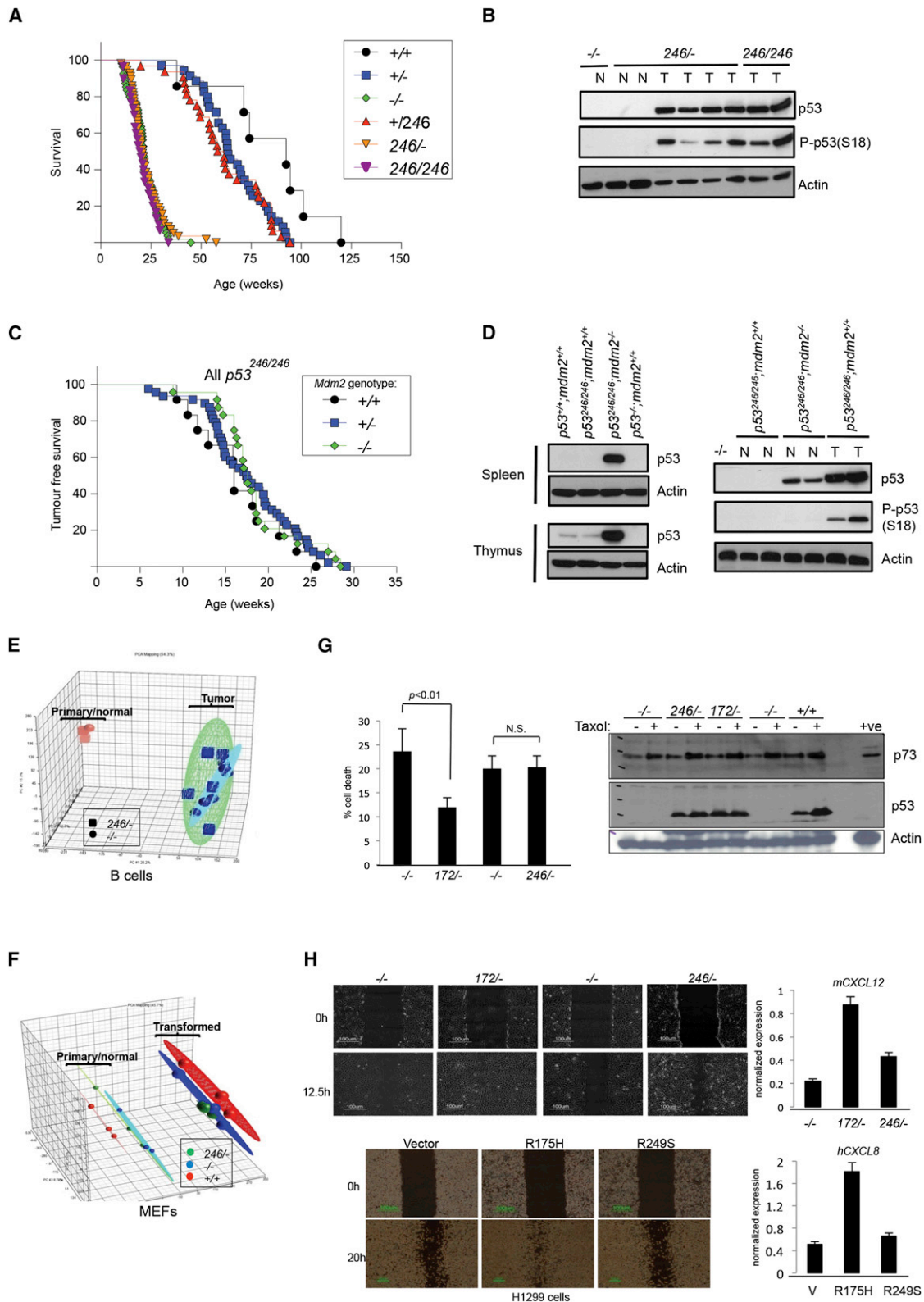
Figure 6. Mutant p53 GOF Properties Are Mutation-type Specific

(A) Kaplan-Meier survival curves of untreated mice of various *p53* genotypes are shown.

(B) Abundance and phosphorylation status of p53 protein in thymoma (T) and normal (N) thymi of mice of various *p53* genotypes were analyzed by western blotting.

Table 1. Characterization of Spontaneous Tumors in Various *p53* Genotypic Backgrounds

p53 Genotype	+/+	+/−	+/246	−/−	246/246
Lymphoma (%)	nd	2/20 (10)	8/19 (42.1)	29/42 (69)	18/23 (78.3)
Sarcoma (%)	nd	19/20 (95)	15/19 (78.9)	10/42 (23.9)	5/23 (21.7)
Other (%)	nd	0/20 (0)	0/19 (0)	3/42 (7.1)	0/23 (0)
Median survival (weeks)	92.43	63.43	59.86	21.29	19.71

Cohorts of mice of various *p53* genotypes were aged, and spontaneous tumor formation was monitored. Moribund mice were sacrificed, and necropsy was performed to determine the type of tumor developed. Stats − (2×2) contingency table of (+/−, +/246) × (lymphoma, sarcoma) (Fisher's exact test): +/− versus +/246, p = 0.0725. Stats − (2×2) contingency table of (+/−, +/246) × (lymphoma, nonlymphoma) (Fisher's exact test): +/− versus +/246, p = 0.031. nd, not detected.

p53 status of the lymphoma cells will be $p53^{-/-}$ and $p53^{R246S/-}$ (Figure S4J). For MEFs, the level of p53 and p19ARF of primary and E1A/Ras-transformed MEFs were determined to ensure transformation was successful (Figure S4K). PCA analyses revealed that the lymphoma cells were distinctly separated from the normal primary B cells (Figure 6E). However, the p53 null and R246S mutant expressing samples were clustered together and not segregated, suggesting the global transcriptome profiles were almost identical. As shown in the volcano plots, the detailed ANOVA comparing p53 null and mutant cells also indicated most genes were not differentially expressed between these two genotypes (Figure S4L). Similar results were obtained using both primary and transformed MEFs, suggesting a lack of GOF properties of the R246S mutant (Figures 6F and S4M). To rule out the possibility that there may be a small collection of genes that may be differentially expressed because of the GOF of the R246S mutant, we determined the expression of genes showing the highest fold changes in the microarray study by qRT-PCR, which did not reveal any differences (Table S1B).

At the cellular level, the viability of $p53^{R246S/-}$ thymocytes was nearly identical to that of $p53^{-/-}$ thymocytes upon irradiation and lacked transactivation potential (Figures 3 and S1D). Moreover, $p53^{R246S/-}$ and $p53^{-/-}$ MEFs always respond similarly to all stresses tested (Figures 2 and 3), further suggesting a lack of GOF at cellular and biochemical levels. Given that the $p53^{R172H/-}$ MEFs have been shown to display GOF properties through the inhibition of its family members (Lang et al., 2004; Olive et al., 2004), we studied the effect on p73-mediated transactivation of target genes upon ectopic expression of p73 in $p53^{R246S/-}$ or $p53^{R172H/-}$ MEFs. Expression of *Mdm2* was much less induced by p73 in $p53^{R172H/-}$ cells compared to $p53^{R246S/-}$ MEFs (Figure S4N). Similarly, p73-mediated upregulation of

p21-promoter luciferase activity was consistently reduced by the R175H but not the R249S mutant, the human equivalents of the mouse mutants examined here (Figure S4O), as previously shown (Gaiddon et al., 2001), suggesting that the R246S mutant p53 is not capable of efficiently inhibiting p73 activity. In order to confirm the lack of this inhibitory activity, we performed two additional experiments. First, we took advantage of the fact that taxol-induced cell death is highly p73-dependent (and not p53-dependent) (Toh et al., 2010) and compared sensitivity of $p53^{-/-}$, $p53^{R246S/-}$, and $p53^{R172H/-}$ MEFs to taxol. Both $p53^{-/-}$ and $p53^{R246S/-}$ MEFs were found to be equally sensitive to taxol treatment, whereas $p53^{R172H/-}$ MEFs were more resistant (percentage of cell death- $p53^{-/-}$ versus $p53^{R246S/-}$ versus $p53^{R172H/-}$: 23.67 or 20.0 versus 20.0 versus 12.0), although p73 induction was similar in all cells (Figure 6G). Next, we analyzed ras-induced cellular transformation, which was shown to be more efficient in $p53^{R172H/-}$ MEFs compared to p53 null cells (Lang et al., 2004). Expectedly, ras-mediated transformation was more efficient in $p53^{R172H/-}$, but not in $p53^{R246S/-}$ MEFs, compared to $p53^{-/-}$ MEFs, resulting in at least 2-fold more colonies in the former case (Figure S4P). Altogether, these data suggest that the inability of R246S mutant to inhibit p73 appears to be one reason for the lack of GOF.

Given that p53 mutants can also exhibit GOF through activation of novel target genes and promote cellular migration (Muller et al., 2009; Weisz et al., 2007, Yeudall et al., 2012), we further examined the effect of R246S mutant on cellular migration. Scratch assays indicated that although the $p53^{R172H/-}$ MEFs were able to close the wounded area fully by 12.5 hr, both $p53^{-/-}$ and $p53^{R246S/-}$ MEFs had only partially migrated (Figure 6H). Similarly, human H1299 cells stably expressing the R175H mutant (Vikhanskaya et al., 2007) were able to close

(C) Kaplan-Meier survival curves of $p53^{R246S/R246S}$ mice on various *Mdm2* genotypic backgrounds are shown.

(D) Western blot analysis of p53 protein levels in normal spleen and thymus (left), and the comparison of p53 levels and phosphorylation status of normal thymi and thymoma from $p53^{R246S/R246S}$ mice of different *Mdm2* genotypes (right) are shown.

(E and F) Transcriptome profiling of tissues/cells of various *p53* genotypes were performed by Affymetrix mouse exon array. Principal component analysis (PCA) is shown for normal and B lymphoma cells from *Eμ-Myc* transgenic mice (E) and for primary and E1A/Ras-transformed MEFs (F). Each data point represents one sample, and the ellipsoids represent the zone within two SD of an experimental group.

(G) Viability of E1A/Ras-transformed MEFs of various *p53* genotypes was determined 48 hr after 400 nM taxol treatment by Annexin v and PI staining (left panel). Respective sibling $p53^{-/-}$ MEFs from the R172H or R246S crosses were used as controls for each mutant-p53 expressing MEF line. Cellular lysates from parallel cultures were used after 24 hr treatment for western blot analysis of p53. p73 expression was determined by immunoprecipitation followed by immunoblotting (right panels). Cells transfected with *p73* was used as a positive control (+ve). Data represents mean ± SEM.

(H) MEFs from the indicated genotypes (top panel) and human H1299 cells stably expressing the indicated p53 mutants (lower panel) were used in wound-healing scratch assays, and photographs taken at 0 hr (at scratch) or the indicated time points thereafter are shown to determine extent of cellular migration. Real-time PCR analysis of mouse (m) *CXCL12* or human (h) *CXCL8* were determined in these cell lines. Data represents mean ± SEM.

See also Figure S4 and Table S1.

Table 2. *Mdm2*^{−/−} Lethality Rescue: Offspring Analysis

p53^{+/246}*Mdm2*^{+/−} Intercross		*p53* +/+	+/246	246/246
Mdm2	+/+	32	77	26
	+/−	78	170	52
	−/−	0	0	22

p53^{+/R246S};*Mdm2*^{+/−} mice were intercrossed to generate mice of various *p53* and *Mdm2* genotypes. Mice were weaned at 3 weeks old, and genotypes were determined by PCR. Numbers in the table indicate number of offspring at 3 weeks of age.

the wounds by 20 hr, at which time the empty vector or R249S mutant p53-expressing counterparts had only partially closed the wounded area (Figure 6H, lower panel). Consistent with these effects, the expression of the chemokines *CXCL12* or *CXCL8*, shown to be novel targets of mutant p53 with GOF (Yeudall et al., 2012), were much more elevated in the *p53*^{R172H/-} MEFs and R175H-expressing H1299 cells, respectively, compared to *p53*^{R246S/-} MEFs and R249S-expressing H1299 cells. These results collectively demonstrate that the R246S p53 mutant, unlike the other hot spot R172H mutant, does not exhibit GOF properties in various cell types, both in the primary and transformed tissues, and even in the absence of Mdm2.

DISCUSSION

The data presented here demonstrate that the DN activity of mutant p53 is indeed operative in vivo. It is apparent after acute p53 activation and affects target gene transactivation and short-term biological outcomes, such as sensitivity to irradiation, in a cell-type-specific manner but does not affect long-term tumorigenesis. Importantly, it is dependent on the dose of the mutant p53, as hypomorphic mice expressing reduced levels of mutant p53 do not exhibit the DN effects. In addition, this study also highlights that the GOF properties of mutant p53 are not a universal phenomenon. It is specific to the mutation and cannot be induced by absence of Mdm2, demonstrating the differences in properties of even the common hot spot mutants found in human cancers. These data raise several interesting points that merit consideration.

First, the DN effect is seen in a cell-type-specific manner, as the biological outcome was affected in embryonic stem cells (Lee and Sabapathy, 2008), T and B lymphoid cells (referred to here as sensitive cell types) but not in Lin^{−} progenitor cells and MEFs (referred to here as insensitive cell types). Interestingly, transactivation was also affected in the insensitive MEFs, indicating that in these cells, p53-mediated target gene transactivation alone may not be sufficient to determine biological outcome, as opposed to the sensitive cell types, in which the p53-dependent target gene activation may the dominant mechanism regulating cellular survival. These findings highlight that mutant p53 is capable of inhibiting the wild-type counterpart at the molecular and biochemical level, although the effect is not translated onto the cellular outcome in all cases. This further suggests that other cell-type-specific and cell fate regulating signaling pathways may be operating in conjunction with p53 pathway, and hence, the manifestation of DN effects on cellular outcome

reflect the reliance of cells on the p53 pathway. Though the identity and nature of factors that discriminate between the cell-type specificity is at present unclear, it appears that the generally observed predisposition of a cell to p53 activation, such as cell-cycle arrest versus apoptosis, is not the determining factor. For example, E1A/Ras-transformed MEFs did not exhibit a DN effect and underwent cell death or cell-cycle arrest upon nutlin treatment and IR, respectively. Moreover, primary MEFs underwent cell-cycle arrest upon nutlin treatment, which induced apoptosis in their transformed counterparts, although a DN effect was not observed in both cases. The manifestation of the DN effect also appears to be independent of cellular "stemness" as the effects were observed in ES cells (Lee and Sabapathy, 2008) but not in Lin^{−ve} hematopoietic progenitors, whereas mature splenic and peripheral lymphocytes displayed the effects.

Second, the DN effect is seen only after acute activation of p53, being able to negate radiosensitivity, but does not appear to contribute to long-term tumorigenesis after irradiation, thereby defining the perimeters for exhibition of the DN effect in vivo. This suggests that the transient activation of p53 activity, which regulates acute cellular survival, is the time point at which the DN effect is manifested, in contrast to baseline activity, which appears to be critical for prevention of tumor formation. The DN effect may therefore be important during therapeutic p53 activation phases, such as during chemo- or radiotherapy. Inducible p53 expression in mice has also supported the notion that p53 activity during acute DNA damage is not sufficient to prevent tumor formation (Christophorou et al., 2006; Junttila and Evan, 2009), emphasizing that the p53 burst in the acute phase of activation is neither relevant nor required for tumor suppressive properties. Supporting this conclusion, a recent study on familial cancer prone patients with different *p53* mutations revealed no differences in the distribution of the clinical subclasses in patients carrying a perceived DN or a severely defective nonfunctional (SD) *p53* allele, suggesting that haploinsufficiency, rather than a DN effect, is the major factor contributing to cancer predisposition (Monti et al., 2011). Interestingly, patients carrying these DN alleles tended to develop brain tumors in contrast to SD allele carriers, who were at a higher risk of developing breast cancers, suggesting tissue specificity of the DN effects in vivo (Monti et al., 2011), as noted in the study presented here.

Another salient point to emerge is that the DN effect is dependent on the dose of mutant p53 protein present in the cells. The DN effect was completely abolished in sensitive cell types in the hypomorphic strain used here, clearly demonstrating the requirement for sufficient levels of mutant p53 to inhibit wild-type p53 function. This is again consistent with the observation that the DN effect is generally seen upon acute p53 activation, when the p53 levels are elevated. While this manuscript was in preparation, Lozano and colleagues showed that reducing wild-type p53 levels in *p53*^{+(Neo)/R172H} mice also led to the manifestation of DN effects in tissues and cell types that generally do not exhibit it (insensitive tissues) (Wang et al., 2011). For example, spontaneous tumor formation was affected by the presence of a weaker wild-type allele. These data provide proof of principle that DN can exist in vivo and are consistent with the fact that the ratio of mutant to wild-type p53 determines the

manifestation of DN effects in sensitive cells, as has also been implied from in vitro work (Chan et al., 2004). In addition, this also suggests that the different mutant p53's may have different properties, including different degrees of the DN effect in the same tissue.

The work presented here implies that the coexistence of mutant *p53* with the wild-type allele prior to LOH will have an impact during acute p53 activation, as shown with the case of radiosensitivity, and thus in cases of therapeutic treatment. Hence, mutant p53 may affect the outcome of treatment, likely leading to reduced or poor response and the eventual relapse of tumors. Though direct clinical evidence for this is unavailable, presence of mutant p53 has been correlated with poor prognosis after treatment (Robles and Harris, 2010). However, one could not be precisely sure if this was due to mutant p53's GOF in tumors that have lost the wild-type allele or to the DN effect of the mutant, as the early sequencing efforts would have not excluded the presence of stromal compartments in evaluating *p53* status (which would contain wild-type *p53* and therefore lead to contamination). We have not been able to directly test the hypothesis that mutant p53's DN effect is indeed contributory to poor response to therapy in mice, as LOH is predominant in tumors arising in the irradiation and the Myc-induced models (data not shown). Nonetheless, evidence from Lozano and colleagues indicate that although wild-type p53 activation in mutant p53-expressing tumors could arrest tumor growth, this is not as efficient as in the case in which mutant p53 is absent, suggesting that mutant p53's presence can indeed prevent complete functionality of wild-type p53 when activated (Wang et al., 2011). Thus, the existence of mutant p53 certainly has a negative impact on cellular survival and hence therapeutic efficacy, either through the DN effect or GOF.

The most convincing evidence by far supporting the existence of GOF in vivo are derived from the analysis of mutant p53 knockin mice harboring other hot spot mutants, such as R172H and R270H, which showed higher incidence of carcinoma and higher metastatic potential than the p53 null mice (Lang et al., 2004; Olive et al., 2004). GOF was attributed to the ability of the mutant p53 protein to inhibit its family members, p73 and p63. However, it is still unclear if GOF properties are universal for all major hot spot mutants and if there are any differences in the degree and spectrum of biological activities of GOF among different mutants. Here, we provide extensive evidence that a particular hot spot mutant may not exhibit GOF in multiple cell types and even when its levels are elevated because of Mdm2 deficiency, challenging the belief that elevated mutant p53 levels alone are sufficient for GOF of all mutants. The lack of GOF properties of the R246S mutant p53 is consistent with its lack of ability to inhibit p73 (this report and Gaiddon et al., 2001), supporting the notion that inhibition of p73 is one mechanism by which GOF is manifested, and highlights the importance of our knockin model in understanding human cancers. Moreover, our data also imply the presence of other negative regulators of p53 abundance, which could be deactivated in the tumor context, leading to further stabilization.

In conclusion, mutant p53 is shown here to have DN effects in a cell-type and dose-dependent manner, especially during acute p53 activation, and hence highlights the need for consideration during cancer therapy. Furthermore, GOF properties

appear not to be a universal phenomenon for all hot spot p53 mutants.

EXPERIMENTAL PROCEDURES

Generation and Breeding of *p53*[+/R246S] Knockin Mice

The targeting construct, screening strategy, targeted mouse generation, and genotyping methodology have been previously described (Lee and Sabapathy, 2008; Lee et al., 2011). All animal experiments were approved by and performed in accordance with the guidelines of the Singhealth's Animal Care and Use Committee.

Cell Culture and Biochemical Analysis

Details of cell/tissue isolation, culture and treatment, cell-cycle and cell death analysis, immunoblotting, flow cytometric, and quantitative real-time PCR analysis are described in detail in the Supplemental Experimental Procedures.

Statistical Analysis

ANOVA was used to determine statistical significance in all experiments, except cancer formation cohorts. Fisher's exact test was used to analyze the difference in incidences of different types of tumor. For cancer formation cohorts, the "Log-rank (Mantel-Cox) test" was used.

ACCESSION NUMBERS

The microarray data reported in this paper have been deposited in the Gene Expression Omnibus (GEO) database (http://www.ncbi.nlm.nih.gov/geo). The accession number is GSE40417.

SUPPLEMENTAL INFORMATION

Supplemental Information includes four figures, one table, and Supplemental Experimental Procedures and can be found with this article online at http://dx.doi.org/10.1016/j.ccr.2012.10.022.

REFERENCES

Bossi, G., Lapi, E., Strano, S., Rinaldo, C., Blandino, G., and Sacchi, A. (2006). Mutant p53 gain of function: reduction of tumor malignancy of human cancer cell lines through abrogation of mutant p53 expression. Oncogene *25*, 304–309.

Brosh, R., and Rotter, V. (2009). When mutants gain new powers: news from the mutant p53 field. Nat. Rev. Cancer *9*, 701–713.

Chan, W.M., Siu, W.Y., Lau, A., and Poon, R.Y. (2004). How many mutant p53 molecules are needed to inactivate a tetramer? Mol. Cell. Biol. *24*, 3536–3551.

Christophorou, M.A., Ringshausen, I., Finch, A.J., Swigart, L.B., and Evan, G.I. (2006). The pathological response to DNA damage does not contribute to p53-mediated tumour suppression. Nature *443*, 214–217.

Gaiddon, C., Lokshin, M., Ahn, J., Zhang, T., and Prives, C. (2001). A subset of tumor-derived mutant forms of p53 down-regulate p63 and p73 through a direct interaction with the p53 core domain. Mol. Cell. Biol. *21*, 1874–1887.

Jackson, E.L., Olive, K.P., Tuveson, D.A., Bronson, R., Crowley, D., Brown, M., and Jacks, T. (2005). The differential effects of mutant p53 alleles on advanced murine lung cancer. Cancer Res. *65*, 10280–10288.

Jones, S.N., Roe, A.E., Donehower, L.A., and Bradley, A. (1995). Rescue of embryonic lethality in Mdm2-deficient mice by absence of p53. Nature *378*, 206–208.

Junttila, M.R., and Evan, G.I. (2009). p53—a Jack of all trades but master of none. Nat. Rev. Cancer *9*, 821–829.

Kemp, C.J., Wheldon, T., and Balmain, A. (1994). p53-deficient mice are extremely susceptible to radiation-induced tumorigenesis. Nat. Genet. *8*, 66–69.

Kern, S.E., Pietenpol, J.A., Thiagalingam, S., Seymour, A., Kinzler, K.W., and Vogelstein, B. (1992). Oncogenic forms of p53 inhibit p53-regulated gene expression. Science *256*, 827–830.

Lang, G.A., Iwakuma, T., Suh, Y.A., Liu, G., Rao, V.A., Parant, J.M., Valentin-Vega, Y.A., Terzian, T., Caldwell, L.C., Strong, L.C., et al. (2004). Gain of function of a p53 hot spot mutation in a mouse model of Li-Fraumeni syndrome. Cell *119*, 861–872.

Lee, M.K., and Sabapathy, K. (2008). The R246S hot-spot p53 mutant exerts dominant-negative effects in embryonic stem cells in vitro and in vivo. J. Cell Sci. *121*, 1899–1906.

Lee, M.K., Tong, W.M., Wang, Z.Q., and Sabapathy, K. (2011). Serine 312 phosphorylation is dispensable for wild-type p53 functions in vivo. Cell Death Differ. *18*, 214–221.

Levine, A.J., Momand, J., and Finlay, C.A. (1991). The p53 tumour suppressor gene. Nature *351*, 453–456.

Lowe, S.W., Ruley, H.E., Jacks, T., and Housman, D.E. (1993). p53-dependent apoptosis modulates the cytotoxicity of anticancer agents. Cell *74*, 957–967.

Milner, J., and Medcalf, E.A. (1991). Cotranslation of activated mutant p53 with wild type drives the wild-type p53 protein into the mutant conformation. Cell *65*, 765–774.

Monti, P., Perfumo, C., Bisio, A., Ciribilli, Y., Menichini, P., Russo, D., Umbach, D.M., Resnick, M.A., Inga, A., and Fronza, G. (2011). Dominant-negative features of mutant TP53 in germline carriers have limited impact on cancer outcomes. Mol. Cancer Res. *9*, 271–279.

Morton, J.P., Timpson, P., Karim, S.A., Ridgway, R.A., Athineos, D., Doyle, B., Jamieson, N.B., Oien, K.A., Lowy, A.M., Brunton, V.G., et al. (2010). Mutant p53 drives metastasis and overcomes growth arrest/senescence in pancreatic cancer. Proc. Natl. Acad. Sci. USA *107*, 246–251.

Muller, P.A., Caswell, P.T., Doyle, B., Iwanicki, M.P., Tan, E.H., Karim, S., Lukashchuk, N., Gillespie, D.A., Ludwig, R.L., Gosselin, P., et al. (2009). Mutant p53 drives invasion by promoting integrin recycling. Cell *139*, 1327–1341.

O'Shea, D., O'Riain, C., Taylor, C., Waters, R., Carlotti, E., Macdougall, F., Gribben, J., Rosenwald, A., Ott, G., Rimsza, L.M., et al. (2008). The presence of TP53 mutation at diagnosis of follicular lymphoma identifies a high-risk group of patients with shortened time to disease progression and poorer overall survival. Blood *112*, 3126–3129.

Olive, K.P., Tuveson, D.A., Ruhe, Z.C., Yin, B., Willis, N.A., Bronson, R.T., Crowley, D., and Jacks, T. (2004). Mutant p53 gain of function in two mouse models of Li-Fraumeni syndrome. Cell *119*, 847–860.

Olivier, M., Hollstein, M., and Hainaut, P. (2010). TP53 mutations in human cancers: origins, consequences, and clinical use. Cold Spring Harb. Perspect. Biol. *2*, a001008.

Oren, M., and Rotter, V. (2010). Mutant p53 gain-of-function in cancer. Cold Spring Harb. Perspect. Biol. *2*, a001107.

Palmero, E.I., Achatz, M.I., Ashton-Prolla, P., Olivier, M., and Hainaut, P. (2010). Tumor protein 53 mutations and inherited cancer: beyond Li-Fraumeni syndrome. Curr. Opin. Oncol. *22*, 64–69.

Petitjean, A., Mathe, E., Kato, S., Ishioka, C., Tavtigian, S.V., Hainaut, P., and Olivier, M. (2007). Impact of mutant p53 functional properties on TP53 mutation patterns and tumor phenotype: lessons from recent developments in the IARC TP53 database. Hum. Mutat. *28*, 622–629.

Robles, A.I., and Harris, C.C. (2010). Clinical outcomes and correlates of TP53 mutations and cancer. Cold Spring Harb. Perspect. Biol. *2*, a001016.

Schmitt, C.A., McCurrach, M.E., de Stanchina, E., Wallace-Brodeur, R.R., and Lowe, S.W. (1999). INK4a/ARF mutations accelerate lymphomagenesis and promote chemoresistance by disabling p53. Genes Dev. *13*, 2670–2677.

Terzian, T., Suh, Y.A., Iwakuma, T., Post, S.M., Neumann, M., Lang, G.A., Van Pelt, C.S., and Lozano, G. (2008). The inherent instability of mutant p53 is alleviated by Mdm2 or p16INK4a loss. Genes Dev. *22*, 1337–1344.

Toh, W.H., Nam, S.Y., and Sabapathy, K. (2010). An essential role for p73 in regulating mitotic cell death. Cell Death Differ. *17*, 787–800.

Varley, J.M., Evans, D.G., and Birch, J.M. (1997). Li-Fraumeni syndrome—a molecular and clinical review. Br. J. Cancer *76*, 1–14.

Vassilev, L.T., Vu, B.T., Graves, B., Carvajal, D., Podlaski, F., Filipovic, Z., Kong, N., Kammlott, U., Lukacs, C., Klein, C., et al. (2004). In vivo activation of the p53 pathway by small-molecule antagonists of MDM2. Science *303*, 844–848.

Vikhanskaya, F., Lee, M.K., Mazzoletti, M., Broggini, M., and Sabapathy, K. (2007). Cancer-derived p53 mutants suppress p53-target gene expression—potential mechanism for gain of function of mutant p53. Nucleic Acids Res. *35*, 2093–2104.

Wang, Y., Suh, Y.A., Fuller, M.Y., Jackson, J.G., Xiong, S., Terzian, T., Quintás-Cardama, A., Bankson, J.A., El-Naggar, A.K., and Lozano, G. (2011). Restoring expression of wild-type p53 suppresses tumor growth but does not cause tumor regression in mice with a p53 missense mutation. J. Clin. Invest. *121*, 893–904.

Weisz, L., Oren, M., and Rotter, V. (2007). Transcription regulation by mutant p53. Oncogene *26*, 2202–2211.

Wijnhoven, S.W., Zwart, E., Speksnijder, E.N., Beems, R.B., Olive, K.P., Tuveson, D.A., Jonkers, J., Schaap, M.M., van den Berg, J., Jacks, T., et al. (2005). Mice expressing a mammary gland-specific R270H mutation in the p53 tumor suppressor gene mimic human breast cancer development. Cancer Res. *65*, 8166–8173.

Wijnhoven, S.W., Speksnijder, E.N., Liu, X., Zwart, E., vanOostrom, C.T., Beems, R.B., Hoogervorst, E.M., Schaap, M.M., Attardi, L.D., Jacks, T., et al. (2007). Dominant-negative but not gain-of-function effects of a p53.R270H mutation in mouse epithelium tissue after DNA damage. Cancer Res. *67*, 4648–4656.

Yeudall, W.A., Vaughan, C.A., Miyazaki, H., Ramamoorthy, M., Choi, M.Y., Chapman, C.G., Wang, H., Black, E., Bulysheva, A.A., Deb, S.P., et al. (2012). Gain-of-function mutant p53 upregulates CXC chemokines and enhances cell migration. Carcinogenesis *33*, 442–451.

Zilfou, J.T., and Lowe, S.W. (2009). Tumor suppressive functions of p53. Cold Spring Harb. Perspect. Biol. *1*, a001883.